European Journal of Neurology

WILEY | ean

REVIEW ARTICLE OPEN ACCESS

Trans-Synaptic Retrograde Retinal Degeneration After Post-Chiasmatic Stroke: A Systematic Review of Empirical Evidence

Francesca Crespi[1,2] | Giacomo Guidali[2] | Lisa Melzi[3] | Stefania Bianchi Marzoli[3] | Nadia Bolognini[2,4]

[1]Ph.D. Program in Neuroscience, School of Medicine and Surgery, University of Milano-Bicocca, Monza, Italy | [2]Department of Psychology, University of Milano-Bicocca, Milan, Italy | [3]Neuro-Ophthalmology Center and Ocular Electrophysiology Laboratory, Scientific Institute Capitanio Hospital, IRCCS Istituto Auxologico Italiano, Milan, Italy | [4]Laboratory of Neuropsychology, Department of Neurorehabilitation Sciences, IRCCS Istituto Auxologico Italiano, Milan, Italy

Correspondence: Francesca Crespi (f.crespi5@campus.unimib.it) | Giacomo Guidali (giacomo.guidali@unimib.it)

Received: 10 November 2025 | **Revised:** 20 February 2026 | **Accepted:** 27 February 2026

Keywords: optical coherence tomography | post-chiasmatic | retina | retrograde trans-synaptic degeneration | stroke

ABSTRACT

Background: Retrograde trans-synaptic degeneration (RTSD) refers to the progressive loss of retinal cells following damage to the post-geniculate visual pathway. The advent of optical coherence tomography (OCT) has allowed the measurement and quantification of retinal layers, in turn providing compelling evidence of RTSD in stroke patients and highlighting that assessing the temporal and functional evolution of RTSD has important clinical implications.

Methods: We conducted a systematic review up until 7th July 2025 to summarize the OCT evidence on post-stroke RTSD. Eligible articles on this topic were searched in PubMed, Web of Science, and Scopus databases. Twenty-eight papers, involving 888 patients and 624 healthy controls, were included, and their results were systematically described and qualitatively analyzed.

Results: Overall, literature shows that RTSD is a frequent outcome of post-chiasmatic strokes. RTSD is operationalized by measuring the thickness of the peripapillary retinal nerve fiber and macular layers. The latter appears to be a more robust structural biomarker, showing more consistent findings across studies, with its magnitude better correlating with patients' visual field defects. RTSD starts early after the stroke's onset and progresses for several years, with severity depending on lesion location and extension. Future investigations are needed to draw more robust conclusions on RTSD temporal dynamics, clarifying the relation between structural and functional loss.

Conclusions: Current literature highlights the need to consider the RTSD among the primary outcomes of post-chiasmatic stroke, given its implications on clinical management and neurorehabilitation, making the longitudinal assessment of this degenerative process crucial for prevention.

1 | Introduction

Stroke is the second leading cause of death and the third leading cause of combined death and disability worldwide [1]. Acquired lesions of the post-chiasmatic visual pathways following stroke, traumatic brain injury, or tumors can result in visual field loss such as homonymous hemianopia or quadrantanopia, that is, a complete or partial loss of the contralesional

Stefania Bianchi Marzoli and Nadia Bolognini shared senior authorship.

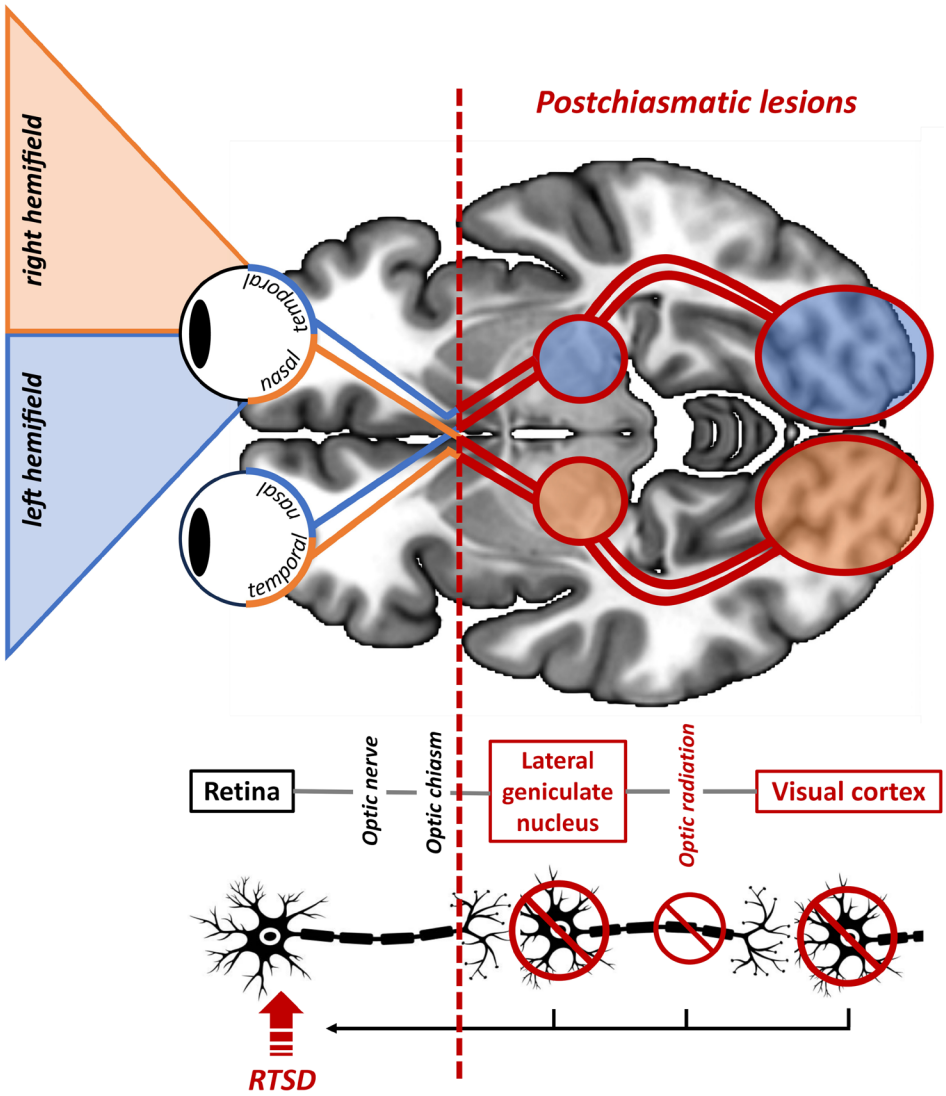

FIGURE 1 | Schematic representation of the visual pathway and post-stroke retinal retrograde trans-synaptic degeneration (RTSD). The present review focuses exclusively on RTSD following post-chiasmatic lesions (i.e., lesions at the level of the primary visual cortex, optic radiation, or lateral geniculate nucleus).

visual hemifield in both eyes. These impairments profoundly impact daily functioning, interfering with activities such as reading, driving, visual searching, and spatial orientation [2, 3].

A growing body of evidence has shown that lesions of the central visual pathways, in addition to the primary visual field defect, also cause retinal degeneration, further damaging patients' vision. This phenomenon, known as retrograde trans-synaptic degeneration (RTSD), involves the progressive loss of retinal ganglion cells following disruption of their post-synaptic targets [4–6] (Figure 1). Unlike pre-geniculate lesions, which cause direct retrograde degeneration of retinal axons and cell bodies, post-geniculate lesions lead to indirect degeneration through trans-synaptic mechanisms. This process is thought to result from the deprivation of neurotrophic support and trans-synaptic signaling. Survival of retinal ganglion cells may depend on stimulus-evoked activity in the primary visual cortex (V1), possibly via direct effects [7], but more likely through indirect mechanisms, mediated by the integrity of intermediate neurons in the dorsal lateral geniculate nucleus (LGN).

RTSD was initially described in animal models after occipital lobectomy [6, 8, 9]. In humans, early histopathological evidence came from rare congenital cases after surgical resection of the occipital lobe [5]. However, it remained debated whether and to what extent RTSD occurs in adults with acquired post-chiasmatic lesions, since optic atrophy was not consistently observed [10]. The advent of optical coherence tomography (OCT) has enabled the non-invasive investigation of this phenomenon.

Introduced in the early 1990s [11], OCT is a non-invasive imaging technique that gives high-resolution cross-sectional images of the retina by analyzing light backscattered from different retinal layers. Initial studies using OCT to investigate RTSD after stroke focused on measuring reduction in the thickness of the peripapillary retinal nerve fiber layer (pRNFL)—composed of unmyelinated retinal ganglion cells axons converging to the optic nerve head e.g., [12]. With subsequent technology

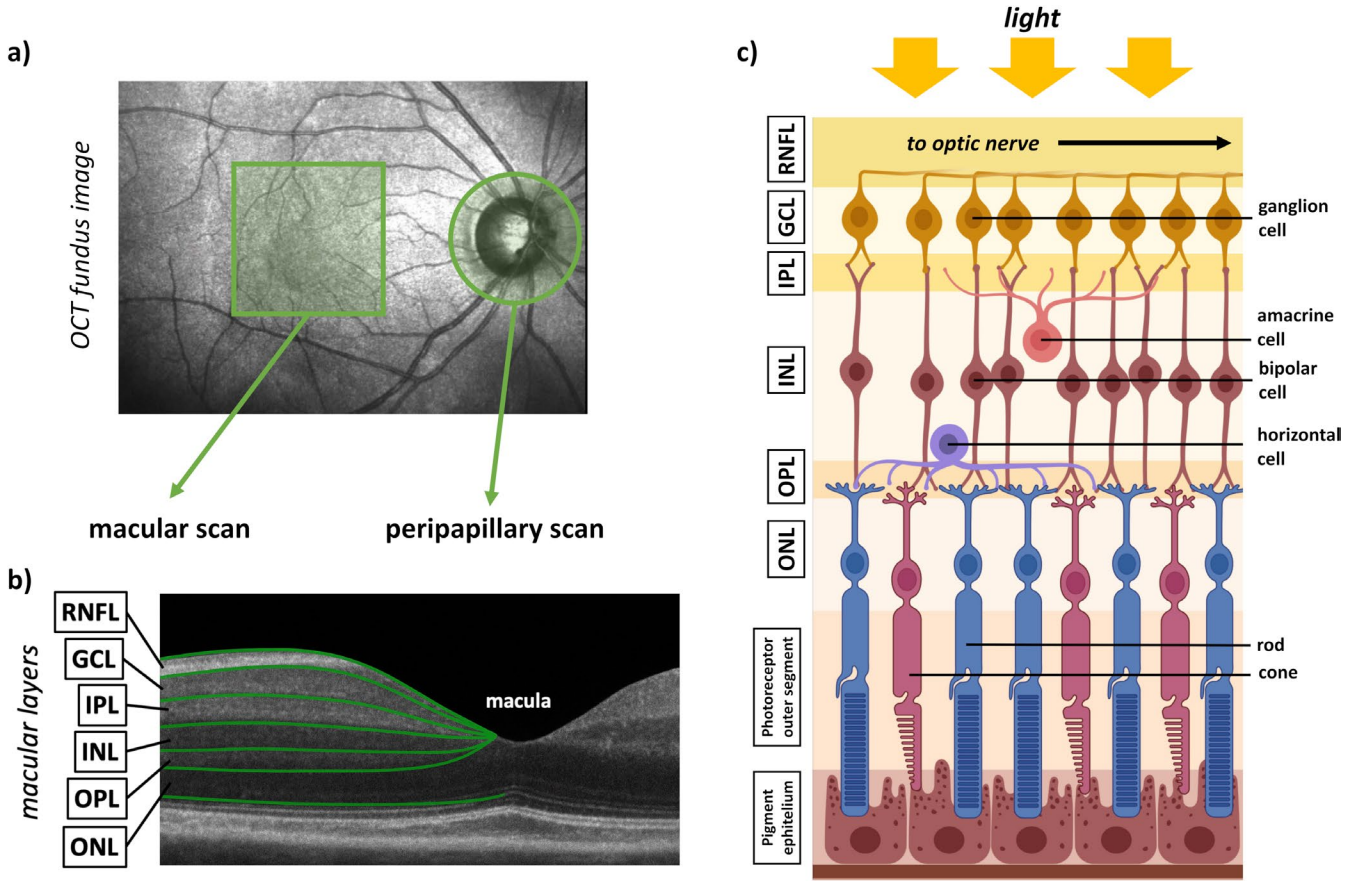

FIGURE 2 | (a) Representative OCT fundus image showing the macular and peripapillary regions. (b) Segmentation of the principal macular layers as assessed through OCT (adapted from [13]). RNFL= retinal nerve fiber layer; GCL= ganglion cell layer; IPL= inner plexiform layer; INL= inner nuclear layer; OPL= outer plexiform layer; ONL= outer nuclear layer. (c) Schematic representation of the retinal structure.

advances, it became possible to segment the macular layers, including the ganglion cell layer (GCL) and the inner plexiform layer (IPL) (Figure 2). According to the specific OCT model, distinct segmentation algorithms and analysis protocols for retinal layer quantification can be implemented. In detail, time-domain OCT (TD-OCT), the earliest generation, provided total macular thickness measurements without true layer differentiation, due to limited axial resolution (~10–15 μm). In contrast, spectral-domain OCT (SD-OCT) is characterized by higher resolution (~5–7 μm) and automated segmentation software capable of isolating specific inner retinal layers, that is, the ganglion cell–inner plexiform layer (GC-IPL), the ganglion cell complex (GCC)—including the RNFL, GCL, and IPL, or the broader inner retinal layer (IRL) – including the GCC and inner nuclear layer (INL) (Figure 2). Again, swept-source OCT (SS-OCT) has improved penetration depth and signal-to-noise ratio, enabling more accurate delineation of deep retinal boundaries and volumetric analysis (e.g., focal volume loss—FLV and global volume loss—GLV). Such analyses allow detailed topographic mapping of retinal thickness and volume, facilitating the identification of retinotopic damage patterns. Finally, OCT angiography (OCT-A) allows the non-invasive visualization of retinal and choroidal vasculature [14].

Given these advantages, OCT is considered the gold-standard technique for investigating retinal and optic nerve-related pathologies, including RTSD [15, 16]. Although the use of OCT to explore RTSD in acquired cerebral lesions is steadily increasing, a systematic review on this topic is still lacking, at variance with similar works in other neurological diseases, where systematic analyses on retinal OCT-derived parameters have already been conducted [14, 17–19]. The present work aims to summarize the current state of the art on OCT assessment of RTSD in post-stroke patients, by reviewing findings on peripapillary and macular parameters, the temporal course of degeneration, the influence of stroke characteristics, the impact on visual function, and the potential implications for rehabilitation.

2 | Methods

We conducted our systematic review in accordance with evidence-based criteria provided by the Preferred Reporting Items for Systematic Reviews and Meta-Analyses (PRISMA 2020) guidelines. We registered it on PROSPERO (International Prospective Register of Systematic Reviews—CRD420251134938).

We systematically searched eligible articles on RTSD in the PubMed, Web of Science, and Scopus databases. The following search string was applied: '(optical coherence tomography) AND ((visual system) OR (vision) OR (occipital) OR (thalamus)

OR (retina)) AND ((stroke) OR (cerebral infarction) OR (ictus))'. No filters regarding publication location or age group of participants were selected in the search process. Literature search was conducted on 7th July 2025.

Two researchers (FC, GG), blinded to each other's choices, independently extracted and selected articles, using Rayyan, an online platform for systematic reviews [20]. Disagreements on the eligibility of a study were resolved by consensus after article screening and selection. Across the three databases, the search yielded 976 papers, which were reduced to 656 after duplicate removal. We subsequently excluded studies that did not fit the aim of the present review. Specifically, we excluded studies if they met at least one of the following criteria:

- Reviews, meta-analyses, or conference abstracts;
- Studies conducted on animal models or in vitro investigations;
- Studies using OCT-A focusing exclusively on vascular measurements;
- Methodological papers addressing OCT parameters, segmentation algorithms, artificial intelligence/deep learning approaches to optimize OCT data acquisition;
- Predictive studies investigating retinal changes as markers of future stroke;
- Studies on pharmacological interventions targeting the eye or visual system;
- Studies investigating pathologic conditions other than retrochiasmatic stroke, including;
  - Non-vascular conditions:
  - Strokes not involving the posterior cerebral artery (PCA) territory, thalamus, or occipital cortex, or studies focusing solely on white matter hyperintensities in the absence of cortical lesions;
  - Maculopathies or non-retrograde retinal degenerations;
  - Case studies on rare genetic or mitochondrial diseases;
- Studies not written in English;
- Studies not published in peer-reviewed journals.

After a full-text eligibility assessment, we excluded 623 articles. A total of 28 papers (24 studies on a clinical population and 4 single-case reports) met the inclusion criteria and were included in the qualitative analysis. The PRISMA flowchart is shown in Figure 3.

For each included study, the following data were extracted and systematically recorded by two reviewers (FC, GG): authors and year of publication; main aim; sample demographics; study design; clinical characteristics (lesion type, site, and timing); visual deficits and OCT model. Table 1 summarizes the extracted data. Due to methodological heterogeneity (see Table 1), statistical analyses on the extracted data were not conducted. Table S1 reports the OCT-related dependent variables analyzed among reviewed studies. We used the PRISMA 2020 reporting guideline [21] to draft this manuscript, and the PRISMA 2020 reporting checklist when editing, included in the Supporting Information.

3 | Results

The reviewed studies included 888 patients and 624 healthy controls. We report the demographics and clinical characteristics of participants in Table 1. Regarding OCT devices, the majority of the studies employed SD-OCT ($n=17$), followed by SS-OCT ($n=6$), TD-OCT ($n=2$), and OCT-A ($n=1$). Two single-case reports did not specify the OCT device used. With respect to primary OCT outcomes related to RTSD, 13 studies reported both macular and peripapillary layers, 5 measured only the pRNFL, and 9 considered solely macular thickness (i.e., mRNFL, GCC, GC-IPL, or IRL). Only 2 studies measured macula's volume-related variables, that is, macular focal loss volume (FLV) and global loss volume (GLV), and one single-case report did not describe quantitative data (See Table S1). Furthermore, 11 studies provided layer thickness data divided by sectors. Sector-specific thickness values, including significant differences, are reported in Table S2.

3.1 | RTSD in Post-Chiasmatic Stroke

3.1.1 | Peripapillary Retinal Nerve Fiber Layer (pRNFL)

Eighteen studies measured the pRNFL thickness in patients with post-chiasmatic lesions (Table S1). Among those with a matched control group (Table 2), most reported a significant pRNFL thinning in patients compared with healthy participants. The reduction involved both the ipsilateral and the contralateral eyes relative to the lesion, with highly significant differences (i.e., $p<0.001$ in several studies) [12, 22–25]. These findings are consistent with those studies that did not include a control group –such as those comparing RTSD in patients with and without visual field defects, or single-case reports—which also demonstrated global pRNFL thinning [13, 26–31]. Some exceptions were observed: Bianchi Marzoli et al. (2023) reported that pRNFL thinning varied according to the affected vascular territory—significant differences compared with controls were found only in patients with parieto-occipital lesions but not occipital ones [32]. Differently, Cavanaugh et al. (2021) and Herro & Lam (2015) found no significant differences in pRNFL thickness [33, 34].

Ten studies further analyzed pRNFL thinning by sectors, quadrants, or clock-hour divisions (Table S2). Most of these works reported significant sectorial thinning, with changes in distribution patterns depending on the eye, ipsilateral or contralateral to the lesion side. Specifically, in ipsilateral eyes, thinning predominantly involved the temporal and supero–/infero-temporal sectors [12, 13, 22, 23, 25, 28, 29], consistent with the involvement of the uncrossed optic chiasm fibers. In contralateral eyes, thinning was more frequently observed in the nasal sectors [12, 22, 25], reflecting the degeneration of crossed optic chiasm fibers. However, results were not entirely consistent across studies. For instance, Rashid et al. (2021) described predominant thinning in the superior and inferior sectors, with no involvement of temporal or nasal regions [27]; Goto et al. (2016) and Gunes et al. (2016) reported no significant differences in the nasal quadrants of contralateral eyes [23, 24], and Yamashita et al. (2012, 2016) observed variable,

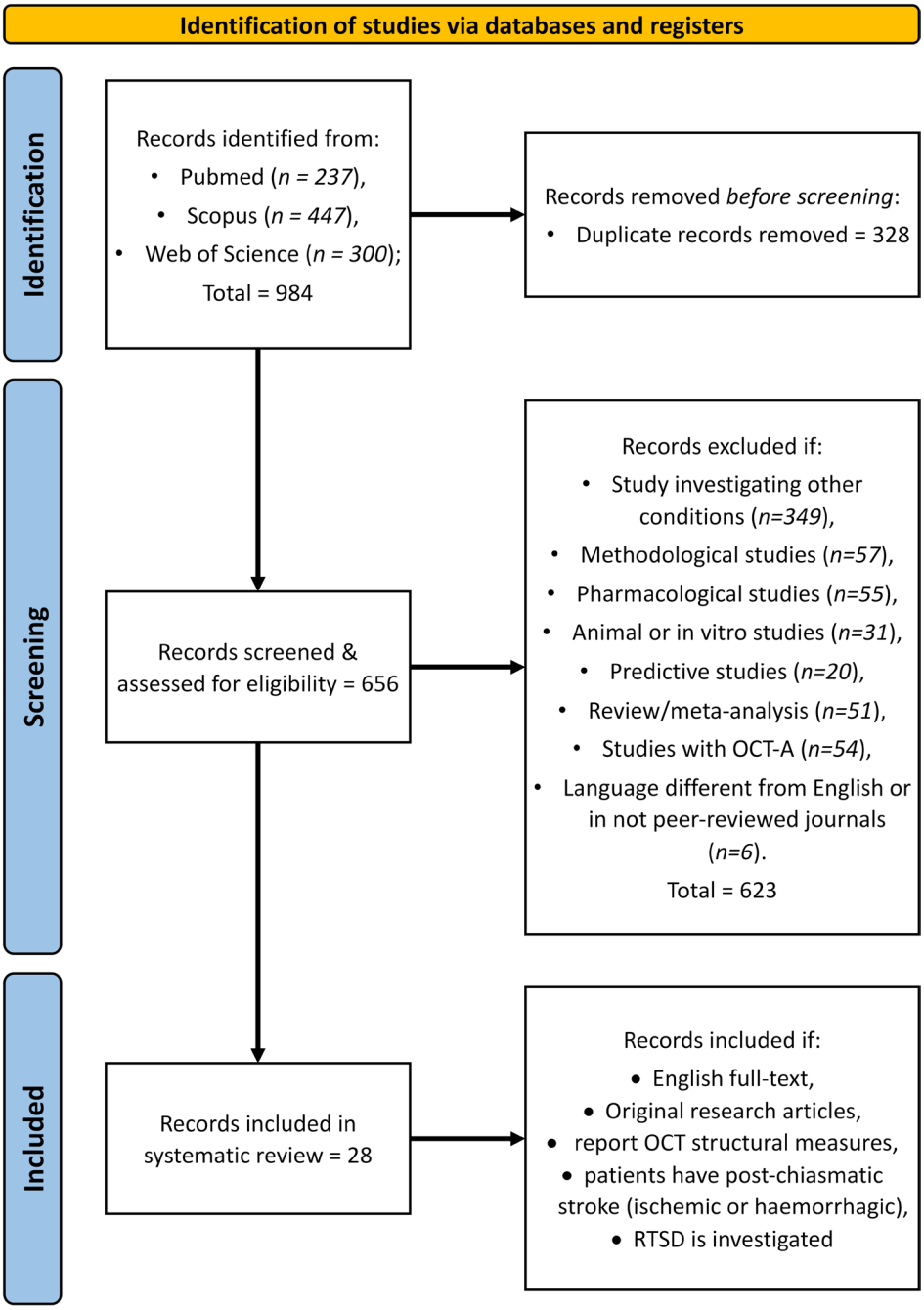

FIGURE 3 | PRISMA flowchart illustrating the literature search and selection process for systematic review.

and not always significant, thinning in nasal sectors of contralateral eyes [28, 29].

3.1.2 | Macular Layer Thickness

Macular layer measurements were reported in 21 studies, but with notable heterogeneity in the parameters assessed. Specifically, 12 studies focused on the GC-IPL, 10 on the GCC, 7 on the RNFL, and only one on the GCL and IRL (Table S1). Despite this variability, most studies documented significant thinning in one or more macular layers in patients compared with controls. However, a few exceptions were reported, e.g., [35, 36] (Table 2). These findings are consistent with reports that did not include a healthy control group—such as single-case reports or longitudinal investigations—which also consistently demonstrated macular layer thinning in stroke patients [13, 26, 27, 29, 31, 34, 36–39].

Nine studies further analyzed macular segmentation by nasal and temporal sectors (Table S1). Across these, a consistent pattern emerged: thinning was typically observed in the temporal sector of the eye ipsilateral to the lesion and in the nasal sector of the contralateral eye when comparing both eyes of the same

TABLE 1 | Summary of extracted data.

Study type	Article	Sample		Experimental design	Stroke type	Stroke site	Time from stroke	Visual deficits	OCT model
		Patients	Healthy controls						
Population study	Jindhara et al. (2009)	26	22 (median 45 years)	Cross-sectional	N/A	Retrogeniculate pathway	Chronic (range: 0.3–67 years)	19 acquired homonymous hemianopia 7 congenital homonymous hemianopia	TD-OCT
	Jindhara et al. (2012)	38 (59.92 years) cross-sectional + 11 longitudinal	23 (43 years)	Cross-sectional + Longitudinal (11 patients)	Cross-sectional: N/A Longitudinal: ischemic ($N=10$), haemorragic ($N=1$)	Cross-sectional: N/A Longitudinal: retrogeniculate pathway ($N=10$), thalamic ($N=1$)	Mixed (range: 6 days—67 years)	Cross sectional: N/A Longitudinal: 7 homonymous hemianopia +4 smaller homonymous VF defects	TD-OCT
	Yamashita et al. (2012)	3 (2 M, 68.3 years)	N/A	Series of case reports	Ischemic	PCA	Chronic (range: 12–36 months)	Homonymous hemianopia	SD-OCT
	Park et al. (2013)	46 (24 M, 55.17 ± 15.26 years)	46 (21 M, 53.4 ± 13.84 years)	Cross-sectional	Ischemic	PCA ($N=17$) MCA ($N=21$) ACA ($N=8$)	Mixed (range: 1–300 months)	N/A	SD-OCT
	Herro & Lam (2015)	9 (8 M, 65.2 years)	N/A	Retrospective	Ischemic	Retrogeniculate pathway	Mixed	Homonymous hemianopia	SD-OCT
	Anjos et al. (2016)	12 (7 M, 66.6 ± 12.7 years)	12 (3 M, 59.1 ± 13.36 years)	Cross-sectional	Ischemic	PCA territory	Mixed (range: 3–156 months)	Homonymous hemianopia	SD-OCT
	Goto et al. (2016)	7 (3 M, 65.7 ± 12.4 years)	49 (15 M, 63.2 ± 7.9 years)	Longitudinal	Ischemic ($N=6$) Haemorrhagic ($N=1$)	PCA ($N=6$) Retrogeniculate pathway ($N=1$)	Chronic (range: 3.5–198.4 months)	2 Inferior quadrantanopia 3 complete hemianopia 2 incomplete hemianopia	SD-OCT
	Gunes et al. (2016)	45 (25 M, 61.6 ± 12.4 years)	45 (28 M, 59.6 ± 11.8 years)	Cross-sectional	Ischemic	PCA MCA	Chronic (mean: 20.2 ± 29.1 months)	N/A	SD-OCT
	Yamashita et al. (2016)	7 (3 M, 62.4 years)	N/A	Cross-sectional	Ischemic Haemorrhagic	PCA	Chronic (range: 1–7.7 years)	6 homonymous hemianopia 1 quadrantanopia	SD-OCT
	Yamashita et al. (2018)	19 (9 M, 60.5 years)	56 (30 M, 56.2 years)	Cross-sectional	N/A	Retrogeniculate pathway (unilateral)	Mixed (range: 0.08–8 years)	Homonymous hemianopia	SS-OCT
	Schneider et al. (2019)	15 (11 M, 63.7 years)	N/A	Prospective	N/A	Retrogeniculate pathway: Occipital ($N=9$, 1 bilateral, 5 right, 3 left) Occipital + other lobes ($N=6$, 1 bilateral, 2 right, 3 left)	Mixed (mean: 10.1 months)	12 homonymous hemianopia 3 quadrantanopia	SD-OCT

(Continues)

TABLE 1 | (Continued)

Study type	Article	Sample		Experimental design	Stroke type	Stroke site	Time from stroke	Visual deficits	OCT model
		Patients	Healthy controls						
	Lee et al. (2020)	21 (11 M, 64 years)	N/A	Longitudinal	Ischemic	Retrogeniculate pathway	Mixed (mean T0: 6.00 ± 3.14 days; mean T1: 176 ± 6.82 days)	N/A	SD-OCT
	Yamashita et al. (2020)	11 (5 M, 65.4 ± 11.4 years)	40 (19 M, 62.3 ± 12 years)	Cross-sectional + Longitudinal (3 patients)	Ischemic ($N = 9$) Haemorrhagic ($N = 2$)	PCA ($N = 9$) Retrogeniculate pathway ($N = 2$)	Mixed (range: 1 month—24.2 years)	9 homonymous hemianopia (6 left, 3 right) 2 quadrantanopia (1 right superior, 1 right inferior)	SD-OCT
	Cavanaugh et al. (2021)	48 (37 M, 59.5 ± 10.2 years)	N/A	Clinical trial	N/A	Retrogeniculate pathway	Mixed (range: 3.4–373.5 months)	Homonymous hemianopia	SD-OCT
	Rashid et al. (2021)	36: 13 VFD (8 M, 70.4 ± 15.3) 23 NVFD (18 M, 67.3 ± 9.0)	N/A	Retrospective + follow up	N/A	Retrogeniculate pathway: Occipital ($N = 14$) Occipital + other lobes ($N = 22$)	Chronic (mean: 24.2 ± 5.8 months)	13 VFD: 5 homonymous hemianopia 5 homonymous quadrantanopia, 3 homonymous scotoma	SD-OCT
	Liang et al. (2022)	159 (120 M, 60.5 ± 11.4 years)	109 (44 M, 58.5 ± 10 years)	Cross-sectional	Ischemic	PCA ($N = 55$) Anterior circulation stroke ($N = 104$)	Mixed (range: 1–372 days)	N/A	OCT-A
	Ye et al. (2022a)	35 (27 M, 59.8 ± 10.7 years)	23 (17 M, 57.9 ± 7.5 years)	Cross-sectional	N/A	Thalamic	Mixed (0.2–44 months)	N/A	SS-OCT
	Ye et al. (2022b)	35 (24 M, 60.26 ± 9.37 years)	31 (20 M, 60.03 ± 6.71 years)	Cross-sectional	Ischemic	Thalamic (unilateral)	Mixed (0.1–8.5 months)	N/A	SS-OCT
	Bianchi Marzoli et al. (2023)	50 (32 M, 61.1 ± 13.3 years)	30 (18 M, 58 ± 13.9 years)	Cross-sectional	Ischemic ($N = 36$) Hemorrhagic ($N = 14$)	Retrogeniculate pathway: Occipital ($N = 15$) Parieto-occipital ($N = 35$)	Mixed (range: 1–348 months)	33 homonymous hemianopia (28/33 complete hemianopia)	SD-OCT
	Donaldson et al. (2023)	15 (64.2 ± 3.5 years)	N/A	Retrospective	N/A	Retrogeniculate pathway: Occipital ($N = 14$) Parieto-occipital ($N = 1$)	Mixed (range: 165–14,600 days)	6 quadrantanopia 9 homonymous hemianopia	SD-OCT
	Fahrenthold et al. (2024)	Same as Cavanaugh et al. (2021) minus 5 patients; $n = 43$ (37 M, 58.9 ± 10.7 years)	N/A	Clinical trial	N/A	Retrogeniculate pathway	Mixed (range: 3.4–373.5 months)	Homonymous hemianopia	SD-OCT

(Continues)

TABLE 1 | (Continued)

Study type	Article	Sample		Experimental design	Stroke type	Stroke site	Time from stroke	Visual deficits	OCT model
		Patients	Healthy controls						
	Pan et al. (2024)	149: 62 thalamic (45 M, 58.58 ± 11.34 years) 87 extra-thalamic (73 M, 55.22 ± 10.05 years)	33 (24 M, 55.97 ± 13.69 years)	Longitudinal	N/A	Thalamic ($N = 62$) Extra-thalamic ($N = 87$) In longitudinal, 30 per patient group	Mixed (range T0: 0.24–10.62 months; range T1: 7.11–21.62 months)	N/A	SS-OCT
	Ye et al. (2024)	46 (33 M, 59.74 ± 10.02 years)	N/A	Cross-sectional	Ischemic	Thalamic (unilateral)	Mixed (range: 1.5–12 months)	N/A	SS-OCT
	Bai et al. (2025)	52 (41 M, 56.94 ± 12.66 years)	105 (85 M, 57.98 ± 9.44 years)	Cross-sectional	N/A	Retrogeniculate pathway	Mixed	N/A	SS-OCT
Single case study	Tanito & Ohira (2013)	87 years, M	/	Single-case report	Ischemic	Right PCA	Chronic (10 years)	Left homonymous hemianopia	SD-OCT
	Schwartz, Monroig & Flynn (2017)	60 years, M	/	Single-case report	N/A	N/A	Mixed (T0: 3 months; T1: 13 months; T2: 17 months)	Left homonymous hemianopia	SD-OCT
	Micieli, Blanch & Narayana (2018)	59 years, W	/	Single-case report	N/A	Right retrogeniculate pathway	Mixed (T0: 100 days; T1: 8 months; T2: 14 months)	Left homonymous hemianopia	OCT
	Eshtiaghi & Micieli (2021)	44 years, M	/	Single-case report	N/A	Left PCA	Acute (1 month)	Right homonymous hemianopia	OCT

Note: Study type; authors and year of publication; sample size (divided for patients and healthy controls, specifying number of subjects, sex distribution, and mean or median age ± SD in years); experimental design, stroke type, stroke site, time from stroke (reported as min-max range or mean ± SD, if available); visual deficits; OCT model used.

Abbreviations: ACA, anterior cerebral artery; MCA, middle cerebral artery; N/A, not applicable or not available; OCT, optical coherence tomography; OCT-A, OCT angiography; PCA, posterior cerebral artery; SD-OCT, spectral domain OCT; SS-OCT, swept source OCT; TD-OCT, time domain OCT.

TABLE 2 | Optic Nerve and Macular OCT parameters in patients compared with healthy controls.

			Optic nerve			Macula						
			pRNFL (μm)			mRNFL (μm)	GCL (μm)		GC-IPL (μm)	GCC (μm)	Volume (%)	
Article	**Experimental group**		**Global**	**Nasal**	**Temporal**	**Global**	**Nasal**	**Temporal**	**Global**	**Global**	**FLV**	**GLV**
Anjos et al. (2016)	Healthy control		102.58 ± 10.3	N/A		N/A	52.21 ± 4.33	47.25 ± 4.38	N/A	N/A	N/A	
	Patients	Hemianoptic side	**79.33 ± 13.54*** **				**45.08 ± 8.49****	**25.92 ± 12.73*** **				
		Controlateral eye	**81.08 ± 11.52*** **				**29.67 ± 12.96*** **	**41.5 ± 8.47***				
Bai et al. (2025)	Healthy control			N/A		37.22 ± 3.55	N/A		67.26 ± 5.43	N/A	N/A	
	Patients					37.86 ± 4.89			**62.3 ± 5.43*** **			
Bianchi Marzoli et al. (2023)	Healthy control		102.6 ± 10.1	N/A		N/A	N/A		N/A	97.3 ± 2.6	0.6 ± 0.5	3.7 ± 1.8
	Patients	Occipital	97 ± 12.1							**89.8 ± 7.2*** **	**2.6 ± 2.5****	**9.7 ± 6.2***
		Parieto-Occipital	**94.8 ± 13.7***							**86.7 ± 8.8****	**3.5 ± 3.2*** **	**12.7 ± 7.4*** **
		Ischemic	96 ± 13.2							**88.3 ± 7.9*** **	**3.1 ± 3****	**11.2 ± 6.5*** **
		Hemorrhagic	94.1 ± 13.4							**85.8 ± 9.9*** **	**3.7 ± 3.2****	**13.5 ± 8.6*** **
Goto et al. (2016)	Healthy control		107.02 ± 6.81	N/A					N/A			
	Patients (controlateral eye)	T0	**97.20 ± 14.11***									
		T1	**95.49 ± 13.46****									
	Patients (ipsilateral eye)	T0	99.93 ± 15.53									
		T1	**98.20 ± 14.02***									
Gunes et al. (2016)	Healthy control		107 ± 7.55	N/A					N/A			
	Patients	Ipsilateral eye	**98 ± 9.26*** **									
		Controlateral eye	**92.2 ± 15.2*** **									
Jindhara et al. (2009)	Healthy control		N/A	101.4 ± 36.6	100.8 ± 35.4				N/A			
	Patients	Acquired		**83 ± 29.5*** **	**79.8 ± 35.1*** **							
		Congenital		**73.4 ± 26****	**72.7 ± 33.2*** **							
Liang et al. (2022)	Healthy control		116.1 ± 12.1	N/A		N/A	N/A		N/A	101.4 ± 6.7	0.7 ± 0.6	1.7 ± 1.8
	Patients (PCA stroke)		112 ± 11.4							96.9 ± 8.5	1.5 ± 1.6	3.5 ± 2.9

(Continues)

TABLE 2 | (Continued)

			Optic nerve			Macula						
			pRNFL (μm)			mRNFL (μm)	GCL (μm)		GC-IPL (μm)	GCC (μm)	Volume (%)	
Article	**Experimental group**		**Global**	**Nasal**	**Temporal**	**Global**	**Nasal**	**Temporal**	**Global**	**Global**	**FLV**	**GLV**
Park et al. (2013)	Healthy control		100.48 ± 13.32	N/A					N/A			
	Patients	Ipsilateral eye	**75.41 ± 14.53*****									
		Controlateral eye	**74.02 ± 13.47*****									
Yamashita et al. (2018)	Healthy control			N/A		28.5 ± 5.3	N/A		82.8 ± 5.6	111.4 ± 8.4	N/A	
	Patients	Hemianoptic side				**24.3 ± 6.2****			**63.7 ± 9.5*****	**86.9 ± 13.7*****		
		Unaffected side				25.8 ± 4.2			73.1 ± 7.9	99 ± 11.4		
Yamashita et al. (2020)	Healthy control			N/A		N/A	N/A		N/A	104.09 ± 4.42	N/A	
	Patients	Hemianoptic side								**83.01 ± 8.05****		
		Unaffected side								88.88 ± 8.43		
Ye et al. (2022a)	Healthy control			N/A		19.286 ± 1.162	N/A		71.277 ± 6.156	N/A	N/A	
	Patients					**17.388 ± 1.759*****			**63.577 ± 8.298****			

Note: The table reports peripapillary (pRNFL) and macular parameters (mRNFL, GCL, GC-IPL, GCC, macular volume) in patients' eyes and controls. For patients, when available, values are specified for the ipsilateral or contralateral (to the lesion) eye. When necessary, data are also divided by lesion location, stroke type, time from stroke, or visual field defect. Nasal and temporal sector values are reported when available; otherwise, only global values are shown. Values are reported as mean ± SD if not otherwise indicated. Bold values indicate statistically significant reductions of retinal layer/volume and asterisks refer to *p*-value of the comparison between patients' and controls' values (if reported in the study).

Abbreviations: FLV, focal loss volume; GCC, ganglion cell complex; GC-IPL, ganglion cell—inner plexiform layer; GCL, ganglion cell layer; GLV, global loss volume; mRNFL, macular retinal nerve fiber layer; N/A, not available; pRNFL, peripapillary retinal nerve fiber layer.

*$p < 0.05$.

**$p < 0.01$.

***$p < 0.001$.

stroke patient [22, 28, 31, 33, 37, 38]. However, some studies diverged from this pattern; for instance, Bai et al. (2025) reported reductions across all macular sectors [35].

3.1.3 | Global Loss Volume (GLV) and Focal Loss Volume (FLV)

Only two studies have examined GLV and FLV parameters (Table 2). Differently from nasal/temporal measures that are anatomically defined across the vertical meridian, focal and global measures are deviation-based and not constrained by hemispheric boundaries. Global metrics reflect average macular loss in the entire region and thus may dilute asymmetric effects; in contrast, focal metrics are more sensitive because they quantify localized deviations. Bianchi Marzoli et al. (2023) reported significantly higher GLV and FLV values in patients compared with controls, with no differences related to the lesion type (ischemic or haemorrhagic) or site (occipital or occipito-parietal) [32]. Similarly, Liang et al. (2022) observed a significant increase in loss-of-volume indices in patients with ischemic stroke compared to healthy controls [36]. However, their cohort included both anterior and posterior vascular territory lesions. Although they did not directly compare patients with posterior lesions against controls, the absence of significant differences between anterior subgroups suggests findings consistent with those reported by [32].

3.2 | Temporal Dynamics of Retinal Degeneration

Several cross-sectional studies investigated the relationship between retinal thinning and time elapsed since stroke (Table 1). By analyzing pRNFL in 3 patients with lesion durations ranging from 12 to 36 months, Yamashita et al. (2012) suggested that ganglion cell degeneration emerges within the first year after stroke [28]. In a subsequent study, the same research group reported a significant linear association between time after stroke and GC-IPL thinning in hemianopic eyes, with thinner layers observed in patients with older lesions [29]. Jindahra et al. (2012) reported that the temporal dynamics of pRNFL loss were better explained by logarithmic regression, with an average decline of approximately 9 μm/log(year), a rate significantly higher than the physiological age-related decline [40]. Similarly, Park et al. (2013) described a logarithmic thinning rate of about 3.3 μm/log(year) [25]. Bianchi Marzoli et al. (2023) confirmed this pattern, reporting logarithmic thinning rates of 8.2 μm/log(year) for pRNFL and 3.5 μm/log(year) for GCC, both significantly greater than those observed in healthy controls [≈0.3 μm/log(year) for pRNFL and no significant GCC change] [32]. Donaldson et al. (2023) further showed that all chronic stroke patients (time since stroke > 30 months) exhibited ≥ 10% relative atrophy of the corresponding macular hemifield, with the earliest detectable onset of RTSD at 5.5 months [39].

Other studies stratified patients according to predefined temporal cut-offs from stroke onset. Liang et al. (2022) compared RTSD in subacute (< 6 months post-stroke) versus chronic (> 6 months post-stroke) ischemic stroke patients [36], while Ye et al. (2022) divided thalamic stroke patients into subgroups based on whether the stroke occurred < 1 month, 1–6 months, or > 6 months before evaluation [30]. However, neither study found significant group differences in retinal layer thickness. Conversely, Bai et al. (2025) investigated retinal macular changes in the acute phase (< 14 days post-stroke), demonstrating that GC-IPL was already reduced compared to controls. In contrast, mRNFL thickness remained unaffected [35] (Table 3).

Only a few studies have examined retinal degeneration longitudinally in the same cohort of patients (Table 3). Jindahra et al. (2012) found that patients with larger homonymous visual field defects, particularly those without macular sparing, exhibited progressive pRNFL thinning, most pronounced within the first 1–2 years post stroke (0.9–6.3 μm/100 days). In contrast, patients with smaller homonymous visual field defects showed no significant changes [40]. Goto et al. (2016) observed that pRNFL thinning in the contralateral (to the lesion) eye was already visible at the baseline (on average, after 50 months from stroke). After 24 months of follow-up, a significant reduction also appeared in the ipsilateral eye [23]. Lee et al. (2020), assessing patients at two timepoints, about 6 days and 6-month post-stroke, reported significant pRNFL reductions [13], in line with previous findings [40]. Similarly, in three patients, Yamashita et al. (2020) found that the mean of GCC values declined progressively over a four-year follow-up, with annual thinning rates ranging from 2.1 to 5.6 μm/year [41].

Evidence from thalamic stroke further supports accelerated retinal degeneration when the lesion involves key relay stations of the visual pathway. Pan et al. (2024) showed that, within the first year after stroke, patients with thalamic infarctions had significantly thinner mRNFL and GC-IPL compared with those with extra-thalamic infarctions. Moreover, the annual rate of GC-IPL thinning was considerably higher in thalamic than in extra-thalamic stroke patients (3.82 vs. 1.90 μm/year) [26].

Finally, two single-case reports described the temporal trajectory of RTSD, suggesting that measurable retinal thinning becomes detectable approximately 1 year after stroke. Schwartz et al. (2017) reported a patient with left homonymous hemianopia whose OCT scans were regular 3 months post-stroke; early GCC thinning appeared at 13 months and further progressed by 17 months [37]. Similarly, Micieli et al. (2018) described a patient with left homonymous hemianopia evaluated at 100 days, 8 months, and 14 months post-stroke. Retinal layer thickness remained stable until 8 months but showed marked bilateral thinning at 14 months [38].

3.3 | Stroke Characteristics Related to RTSD

Regarding stroke type, 10 studies included only ischemic lesions, 4 included both ischemic and haemorrhagic strokes, and 14 did not specify the lesion type (Table 1). Bianchi Marzoli et al. (2023) directly compared retinal layer thickness between ischemic and haemorrhagic strokes, reporting that both groups showed significant differences in GCC, FLV, and GLV values compared with controls, but no significant differences between stroke aetiologies [32].

TABLE 3 | OCT parameters in patients, stratified by time from stroke.

			Optic nerve	Macula													
			pRNFL (μm)	mRNFL (μm)				GC-IPL (μm)				GCC (μm)		IRL (μm)		Volume (%)	
Article	Experimental group		Global	Global	Relative change/ years	Nasal	Temporal	Global	Relative change/ years	Nasal	Temporal	Global	Relative change/ years	Nasal	Temporal	FLV	GLV
Bai et al. (2025)	< 14 days		N/A	38.21		N/A		60.75		N/A		N/A		N/A		N/A	
	> 14 days			37.59				**63.51***									
Donaldson et al. (2023)	Patients		N/A			N/A				N/A		N/A	6.1 ± 5.64	N/A		N/A	
Goto et al. (2016)	Patients (controlateral eye)	Initial visit	97.20 ± 14.11							N/A							
		After 24 months	95.49 ± 13.46														
	Patients (ipsilateral eye)	Initial visit	99.93 ± 15.53														
		After 24 months	98.20 ± 14.02														
Lee et al. (2020)	T0		N/A	N/A		47.28 ± 8.53	19.35 ± 1.69	N/A		68.65 ± 5.98	68.91 ± 6.98	N/A		115.48 ± 12.27	88.22 ± 7.25	N/A	
	T1					**44.36 ± 6.48***	19.19 ± 1.77			68.97 ± 6.35	71.06 ± 12.04			**112.93 ± 10.57***	87.57 ± 7.89		
Liang et al. (2022)	Early stroke (t < median stroke duration)		112.32 ± 13.83			N/A				N/A		98.05 ± 8.23	N/A	N/A		1.06 ± 1.1	3.23 ± 3.06
	Late stroke (t > median stroke duration)		114.23 ± 11.19									99.39 ± 8.71				1.38 ± 1.46	2.75 ± 2.76
Pan et al. (2024)	Thalamic stroke		N/A	N/A	0.255 (−0.015–0.525)	N/A		N/A	3.816 (2.978–4.653)	N/A		N/A		N/A		N/A	
	Extra-thalamic				0.275 (0.099–0.45)				**1.895 (1.314–2.476)*****								
Ye et al. (2022a)	Patients (controlateral eye)	≤ 6 months	95.11 ± 18.48	17.78 ± 1.46		N/A		62.14 ± 7.19		N/A		N/A		N/A		N/A	
		> 6 months	97.88 ± 15.35	17.59 ± 1.85				63.8 ± 10.64									
	Patients (ipsilateral eye)	≤ 6 months	95.5 ± 19.56	17.40 ± 1.54				61.44 ± 8.17									
		> 6 months	97.8 ± 14.67	17.65 ± 1.98				64.52 ± 8.58									
Ye et al. (2022b)	< 1 month		N/A	16.94 ± 1.463		N/A		61.667 ± 8.131		N/A		N/A		N/A		N/A	

Note: The table reports optic nerve (pRNFL) and macular parameters (mRNFL, GC-IPL, GCC, IRL, macular volume) across reviewed studies. Data are stratified according to the time elapsed since the stroke. Data from ipsilateral and contralateral eyes (to the lesion) are also included when specified. Nasal and temporal sector values are reported when available, in addition to or alternative to global values. Values are reported as mean ± SD if not otherwise indicated. Bold values indicate statistically signfiicant reduction of retinal layer/volume and asterisks refer to the p-value of the comparison between time points or groups divided by stroke duration (if reported in the study).
Abbreviations: FLV, focal loss volume; GCC, ganglion cell complex; GC-IPL, ganglion cell—inner plexiform layer; GLV, global loss volume; IRL, inner retinal layers; mRNFL, macular retinal nerve fiber layer; N/A, not available; *P*, patients; pRNFL, peripapillary retinal nerve fiber layer.
*$p < 0.05$.
***$p < 0.001$.

TABLE 4 | OCT parameters according to lesion site and visual field defects.

				Optic nerve	Macula				
				pRNFL (μm)	mRNFL (μm)	GC-IPL (μm)	GCC (μm)	Volume (%)	
Study type	**Article**	**Experimental Group**		**Global**	**Global**	**Global**	**Global**	**FLV**	**GLV**
Lesion site	Bianchi Marzoli et al. (2023)	Occipital		97 ± 12.1	N/A	N/A	89.8 ± 7.2	2.6 ± 2.5	9.7 ± 6.2
		Parieto-Occipital		94.8 ± 13.7			86.7 ± 8.8	3.5 ± 3.2	12.7 ± 7.4
	Gunes et al. (2016)	MCA		95.8 ± 13.7	N/A				
		PCA		92.8 ± 9.3					
	Liang et al. (2022)	Anterior circulation stroke		114 ± 13.1	N/A	N/A	99.7 ± 8.4	1.1 ± 1.1	2.7 ± 2.9
		Posterior circulation stroke		112 ± 11.4			**96.9 ± 8.5***	1.5 ± 1.6	3.5 ± 2.9
	Pan et al. (2024)	Thalamic		N/A	19.36 ± 2.09	73.66 ± 9.34	N/A	N/A	
		Extra-thalamic			**20.20 ± 1.79***	**77.29 ± 7.87***			
Visual field deficit	Donaldson et al. (2023)	Hemianoptic	Hemianopic side	66.56 ± 14.41	N/A				
			Unaffected side	77.73 ± 8.73					
		Quandrantoptic	Hemianopic side	63.33 ± 7.98					
			Unaffected side	78.5 ± 8.86					
	Rashid et al. (2021)	Visual Field Deficit	Left eye	77.3 ± 7	N/A	64.5 (62–71.3)	N/A	N/A	
			Right eye	78.9 ± 8.1		61.5 (50–67.8)			
		No Visual Field Deficit	Left eye	**88 ± 7.4****		**78 (74.5–83.8)****			
			Right eye	**89 ± 6.7****		**81 (74.8–84)****			

Note: The table reports optic nerve (pRNFL) and macular parameters (mRNFL, GC-IPL, GCC, FLV, GLV) across the reviewed studies. Global values without sectoral division are presented. Data are stratified by lesion site (occipital, parieto-occipital, middle cerebral artery, posterior cerebral artery, anterior circulation, posterior circulation, thalamic or extra-thalamic) and by visual field defect (hemianopia, quadrantanopia, or no visual field defect). When specified, comparisons between hemianopic-affected vs. unaffected hemifield and right vs. left eye are also reported. Values are reported as mean ± SD, if not otherwise indicated. Bold values indicate statistically significant reduction of retinal layer/volume and asterisks refer to the *p*-value of the comparisons between different lesion sites or visual field defects (if reported in the study).

Abbreviations: FLV, focal loss volume; GCC, ganglion cell complex; GC-IPL, ganglion cell—inner plexiform layer; GLV, global loss volume; MCA, middle cerebral artery; mRNFL, macular retinal nerve fiber layer; N/A, not available; PCA, posterior cerebral artery; pRNFL, peripapillary retinal nerve fiber layer.

*$p < 0.05$.

**$p < 0.01$.

Regarding the site of the post-stroke damage, 13 studies specifically reported involvement of the retrogeniculate pathway (including the occipital cortex), 8 involved lesions within PCA territory, 2 included both PCA and post-chiasmatic lesions, 4 focused selectively on thalamic strokes, and one did not specify lesion site (Table 1).

Three studies directly compared OCT measures between patients with PCA strokes and those with lesions in other vascular territories (Table 4). Park et al. (2013) reported the greatest pRNFL loss in PCA infarctions, followed by middle cerebral artery (MCA) and anterior cerebral artery (ACA) strokes [25]. Similarly, Liang et al. (2022) found that PCA infarcts were associated with significant GCC thinning compared with anterior circulation strokes, although pRNFL differences did not reach significance [36]. Gunes et al. (2016) found no significant differences in OCT measures between PCA and MCA infarcts [24]. Focusing on thalamic strokes, Pan et al. (2024) reported greater mRNFL and GC-IPL thinning in thalamic lesions compared to extra-thalamic strokes [26].

Three studies examined the relationship between lesion size and the extent of retinal degeneration. Bianchi Marzoli et al. (2023) found no significant differences between isolated occipital and occipital-parietal strokes, although raw values suggested a trend toward greater thinning in the latter group (Table 4) [32]. Conversely, Bai et al. (2025) identified a significant negative correlation between GC-IPL thickness and lesion diameter [35]. Similarly, Ye et al. (2022) reported that thalamic lesion size correlated positively with impairment of macular microvasculature and structural RTSD severity—indicating that greater lesion extension was associated with more pronounced retinal degeneration [30].

3.4 | Relation Between Visual Field Defects and RTSD

Except for 9 studies, all the others reported stroke-related visual defects, typically assessed through perimetry (Table 1). Only one study directly compared patients with and without visual field defects, showing that average GC-IPL and pRNFL thickness were significantly reduced exclusively in patients with concurrent visual field loss [27].

Several studies examined the potential correlation between retinal thinning and quantitative measures of visual field impairment derived from perimetry, although results were inconsistent across reports. Goto et al. (2016) found that pRNFL thickness correlated with mean deviation (MD) and hemianopic total deviation (H-TD) in quadrant-specific analyses, but only after 24 months from the initial evaluation [23]. Similarly, Yamashita et al. (2020) reported quadrant-specific correlations between pRNFL thinning and perimetric variables (i.e., MD/H-TD values), reporting linear or polynomial relationships between GCC thinning and visual field loss in the hemianopic eye [41]. Using voxel-based lesion symptom mapping, Schneider et al. (2019) demonstrated that lesions involving the ventral primary visual cortex or Meyer's loop were associated with greater GCC thinning in region corresponding to the upper visual field, while lesions affecting Baum's loop were associated with greater thinning in areas representing the lower visual field—thus confirming a spatial correspondence between GCC thinning and visual field deviation. However, Bianchi Marzoli et al. (2023) and Donaldson et al. (2023) found no significant associations for pRNFL or GCC thickness [32, 39].

3.5 | Impact of Visual Training on RTSD: the Slowing Effect

To date, the studies by Cavanaugh et al. (2021) and Fahrenthold et al. (2024) are the only investigations exploring whether daily visual perception training could slow the progression of RTSD following occipital stroke [34, 42]. Patients underwent approximately 6 months of visual motion discrimination training. Two groups were compared according to the spatial location of visual stimulus presentation during the task—within the blind hemifield (target group) or at the corresponding location in the intact hemifield (control group). Outcome measures included perimetric MD and retinal layer thickness, with a laterality index computed for GC-IPL and pRNFL to account for baseline inter-ocular thickness variability. Cavanaugh et al. (2021) reported that patients trained within the blind hemifield exhibited systematic improvements in MD compared with those trained in the intact field, but did not observe significant training-related effects on retinal thickness measures [34]. Subsequently, Fahrenthold et al. (2024) analyzed the same sample, excluding five patients with unreliable pre- and post-training Humphrey visual fields, and combined data from both eyes into a single per-patient measure for both perimetric and OCT outcomes, reducing inter-individual variability in retinal thickness and increasing sensitivity to detect change. With these analyses, they found that patients trained within the blind hemifield showed improvements in both MD and average blind-field sensitivity, while the GC-IPL laterality index became significantly more positive only in patients trained in the intact hemifield, indicating greater progression of thinning when the defective hemifield remained untrained. No significant changes in pRNFL thickness were found in either group, instead. This has been attributed by the authors to the anatomical complexity of the RNFL across peripapillary zones, its relatively small volume, inter-individual variability, and the limited sample size, which may have reduced the ability to detect potential changes [42]. Overall, these preliminary findings underline the potential of perceptual training in the blind hemifield for contrasting the progression of RTSD, particularly at the level of the macular layers.

4 | Discussion

The present systematic review provides converging evidence that RTSD occurs in patients with post-chiasmatic stroke and can be reliably detected using OCT.

The degeneration of peripapillary layers was historically the first manifestation of RTSD to be documented after post-chiasmatic lesions. Indeed, the first OCT study to demonstrate RTSD in acquired lesions was by Jindahra et al. in 2009, reporting pRNFL thinning in both congenital and acquired cases, with no

significant differences between groups. In the following decade, multiple cross-sectional and longitudinal studies confirmed progressive pRNFL thinning after stroke, typically showing a sectorial pattern reflecting the topographical organization of crossed and uncrossed fibers at the optic chiasm. Specifically, thinning of the superior and inferior sectors was observed in the eye ipsilateral to the lesion (the "non-crossing fiber defect" eye), and nasal thinning in the contralateral eye (the "crossing fiber defect" eye). For instance, a left occipital lesion causing right homonymous hemianopia would correspond to superior and inferior pRNFL thinning in the left eye and the nasal thinning in the right eye. Nevertheless, other studies have reported discordant findings, including nasal thinning in the ipsilateral eye and temporal thinning in the contralateral eye [23, 24, 28]. Such variability likely reflects sample heterogeneity and methodological differences in sector division (e.g., 6 vs. 12 sectors [22]). Moreover, several reports found no significant differences compared with controls, suggesting that pRNFL may not represent the most sensitive or reliable measure of RTDS [33, 34].

With the advent of SD-OCT, it has also become possible to explore macular layers, which contain the neuronal cell bodies of retinal ganglion cells [19, 43]. Compared with pRNFL, macular parameters appear less influenced by confounding factors such as age, refractive error, and ethnicity [44], and are less likely to be masked by disc swelling or structural anomalies [45]. Indeed, multiple studies have demonstrated that macular measurements are more reliable than peripapillary indices for detecting nerve fiber damage in homonymous hemianopia [28, 31–33, 41]. Although substantial variability exists among studies regarding which layers were analyzed and which OCT models were used (Table S1), nearly all investigations documented progressive macular thinning after post-chiasmatic lesions. Unlike the complex anatomical organization of peripapillary fibers, macular neurons are topographically arranged according to the visual field, allowing more straightforward correspondences between the nasal and temporal macular sectors and the affected hemifield [22, 31, 33, 37]. For instance, a left occipital lesion producing right-sided visual field loss would be expected to cause thinning in the right eye's nasal macular sectors and the left eye's temporal sectors. This retinotopic relationship is closely related also to the distribution of retinal ganglion cell types, particularly parvocellular (P) and magnocellular (M) cells, which differ in function and retinal location. P cells, specialized for mediating high-resolution color and form vision, are small in size and more concentrated in the central retina. Their axons mostly contribute to the temporal portion of the optic nerve head. In contrast, M cells, specialized for the processing of coarser, rapid, transient processing of visual information (low spatial frequency, high temporal frequency), are larger, more widely distributed across the peripheral retina, and their axons course mainly through the superior, inferior and nasal sectors of the optic nerve head [46–48]. Studies in animal models have shown that following occipital lesions, retrograde degeneration affects mainly ganglion cells projecting to the parvocellular layers of the LGN, while M cells are relatively spared, especially those in the peripheral retina [49, 50]. This selective damage suggests that post-geniculate trans-synaptic degeneration primarily involves central retinal regions. Consistent with these findings, studies summarized in this review demonstrate a greater thinning of the central macular retina where P-cells are most concentrated. In contrast, the nasal peripapillary RNFL of contralateral eyes is often relatively preserved. This supports the hypothesis that RTSD respects the retinotopic distribution of retinal ganglion cell subtypes, resulting in a close relationship between the location of ganglion cell loss and the retinotopic representations damaged in the visual cortex.

Considering the temporal chronometry of RTSD, retinal thinning begins within the first months after stroke, becomes evident after approximately 1 year, and may continue for several years [39]. However, some inconsistent findings are reported, such as the study by Bai et al. (2025), which showed retinal degeneration as early as 14 days post-stroke—that is, with a timing much shorter than the typically observed for RTSD. An explanation for this early degeneration is that these retinal changes may reflect direct involvement of the LGN or optic tract, as these structures receive blood supply from the anterior and lateral choroidal arteries, mimicking the retinal pattern of RTSD even if they are instead caused by retinal ischaemia. Accordingly, some studies described a linear relationship between time since stroke and retinal thinning [29, 41], while others reported a logarithmic trajectory characterized by faster initial loss followed by slower progression [25, 32, 40]. Estimated thinning rates ranged from approximately 3–9 μm/log (year) for the pRNFL and 2–5 μm/log (year) for the GCC or GC-IPL [25, 32, 39–41]. These values, however, are only indicative due to the high variability in sample characteristics, follow-up times, and methodologies across studies. Nevertheless, RTSD progression appears significantly faster than physiological age-related thinning observed in healthy controls [≈0.3 μm/log(year)] for pRNFL and no significant GCC change [32, 40]. Longitudinal studies and single-case reports align with this pattern, although the rate of degeneration may vary according to visual field defect size and the presence of macular sparing [40]. Only one study specifically addressed the time course of RTSD after a thalamic stroke, showing faster retinal degeneration than extra-thalamic lesions [26].

The timing of degeneration may also help explain the discrepant findings between studies. Indeed, given the progressive and time-dependent nature of RTSD, the absence of detectable peripapillary or macular thinning sometimes reported may be due to OCT assessments performed too early after the stroke event, before transsynaptic retinal degeneration occurred and, hence, became detectable with OCT. Moreover, recent evidence has quantitatively investigated the progression of visual field defects after stroke, confirming that, in the subacute phase, the spontaneous recovery is greater, likely due to the edema resolution and post-stroke inflammation. Later, approximately one-third of chronic patients continue to show improvement, while a fifth get worse. Interindividual variability plays a central role in the evolution of the visual field defect. In the subacute stage, worsening may result from a prolonged pathological state or comorbidities (e.g., glaucoma, cerebrovascular small vessel disease, or systemic vascular risk factors), whereas in the chronic phase it is more likely related to progressive RTSD. Initially, this degeneration involves visual structures corresponding to the primary lesion, but then it may extend over time, potentially contributing to a progressive enlargement of the perceptual deficit measured by perimetry [51, 52].

Some evidence suggests that the severity of RTSD may be influenced by lesion characteristics such as location, size, and type. Most studies indicated that infarctions in the visual pathway—particularly to the PCA territory or thalamus—result in more pronounced macular and peripapillary thinning than lesions in other vascular territories (e.g., ACA and MCA) and extrathalamic sites [25, 26, 36]. In contrast, Gunes et al. (2016) did not observe significant differences between PCA and MCA strokes, possibly due to small sample sizes or variable disease duration [24]. Regarding the extent of the injury, Bianchi Marzoli et al. (2023) found no differences between lesion circumscribed to the occipital lobe, and those extending to parietal areas [32], while others reported correlations between lesion volume and retinal layer thinning [30, 35]. The only study comparing ischemic and haemorrhagic strokes found comparable retinal thinning across aetiologies, with no specific effect of stroke type differences between the two groups in GCC thickness depending on the stroke type [32]. These findings suggest that lesion size and location influenced RTDS severity.

Finally, the functional consequences of RTSD have been explored by correlating the retinal layer thickness with the extent of campimetric visual field loss, but the results appear inconsistent. Some studies found significant correlations between perimetric indices and macular or peripapillary parameters [7, 23, 41], supporting a spatial correspondence between structural and functional loss. Other investigations, however, failed to detect such associations [32, 39], suggesting that the magnitude of visual field impairment does not always predict the degree of retinal thinning. Differences in the types of perimetry employed and in their spatial correspondence with OCT measurements, which in some cases represent only a limited portion of the central visual field, may explain these inconsistencies. These discrepancies highlight the need for larger and more representative samples, including patients with partial or localized defects (e.g., quadrantanopia or scotomas), and for studies integrating OCT-derived structural indices with perimetric measures to improve the characterization and prediction of post-geniculate visual dysfunctions.

Assessing the presence and extent of RTSD after post-chiasmatic stroke has several important clinical implications e.g., [53]. First, OCT provides an objective structural biomarker of posterior visual pathway damage, complementary to perimetry, and allows disease progression to be monitored over time. Furthermore, perimetry highly depends on patients' cooperation, making it unreliable in severely impaired individuals, at variance with OCT, which is a passive examination, not requiring overt responses from the patient. Second, quantifying RTSD may have prognostic value for rehabilitation. Rehabilitation programs targeting blind-field regions that have not yet undergone RTDS may yield better outcomes, as these areas likely correspond to preserved cortical activity [7]. Conversely, advanced retinal degeneration may limit the potential for training-induced recovery, underscoring the need for early intervention. Third, RTSD could represent a potential therapeutic target for neuroprotective or rehabilitative interventions e.g., [54]. Indeed, at present, rehabilitation approaches for visual field defects due to post-chiasmatic lesions include restorative or compensatory treatments [2, 55, 56]. Restitutive treatments based on perceptual learning aim to expand the visual field through intensive stimulation of the so-called transition zone between intact and blindfield regions [57–59]. On the other hand, compensatory treatments aim to improve oculomotor strategies by training saccadic eye movements [60–64]. More recently, some evidence suggests that integrating behavioral training with non-invasive brain stimulation techniques, such as transcranial direct current stimulation [65, 66], transcranial alternating current stimulation [67], transcranial random noise stimulation [68] or paired associative stimulation [69], can enhance training-induced plasticity, in turn maximizing the effectiveness of behavioral treatment. However, as reviewed here, only two studies to date have investigated whether visual rehabilitation can also influence the progression of RTSD measured by OCT. In particular, Fahrenthold et al. (2024) demonstrated that an intensive perceptual training, consisting of a daily motion direction discrimination task near the border of the visual deficit with attention-guiding cues and adaptive difficulty, may slow or partially prevent degeneration. This effect is thought to result from direct stimulation of surviving retinal cells in areas deprived of cortical input, thereby increasing their metabolic activity and that of their surrounding supporting cells, such as Muller glia, which contribute to the structural stability of the retina [42]. Further studies are needed to explore the influence of retinal degeneration on rehabilitation efficacy, and viceversa.

Several limitations should be acknowledged. Many studies included small and heterogeneous samples, presenting patients with variable lesion ages, types, sizes, locations, and comorbidities such as hypertension or diabetes. Most investigations were single-centre, limiting the generalizability. Stronger conclusions regarding the temporal dynamics of RTDS are precluded by the small number of truly longitudinal studies or by variability in follow-up timing [13, 23, 37, 40, 41]. Differences in OCT models, segmentation algorithms, and the analyzed retinal layers also limited quantitative comparison across studies. Altogether, such variability complicates the interpretation of results and limits the strength of conclusions. To address this, future studies could preferably employ macular rather than peripapillary measures, given their closer retinotopic correspondence with visual field defects and their lesser susceptibility to confounding factors. In addition, to further improve the interpretation of post-chiasmatic stroke effects, it would be interesting to develop an OCT analysis that allows the comparison not only of the superior and inferior hemifields, but also of the nasal and temporal macular hemifields. In this way, in addition to standard measures of retinal layer thickness derived from OCT, indexes could be also derived that take greater account for inter-individual baseline thickness variance, as already done recently with promising findings for example, [42]. Moreover, future studies are also necessary to better understand the relationship between RTSD and other secondary consequences of damage to the visual pathways as microcystic macular oedema. Notably, to our knowledge, this pathology has never been reported following isolated LGN lesions, consistent with early animal studies and suggesting that central post-geniculate damage alone does not produce cystic changes in the retina [70]. Finally, because this review focused exclusively on post-chiasmatic stroke, we excluded studies including mixed etiologies (e.g., stroke, tumor, or traumatic brain injury). These studies, however, found results

in line with the present review, reporting a significant degeneration of retinal layers, especially at the macular level, when lesions involved post-chiasmatic sites [45, 71–73].

As a final note, we highlight that OCT provides indications of retinal layer thickness but does not allow for distinguishing between retinal ganglion cell death and shrinkage of the cell body or dendritic field. However, RTSD has been interpreted as a progressive process that ultimately leads to retinal ganglion cell loss over time. Studies on the timing of RTSD show that it becomes evident within the first months after injury, suggesting that interventions aimed at preserving retinal ganglion cells are likely to be most effective when applied early. In contrast, once there is a marked thinning of the ganglion cells within a given retinotopic sector, it is more conceivable that restoring vision at that location would be unlikely, as the afferent visual input is substantially reduced or absent. In line with this, a recent study by Fahrenthold et al. (2021) assessing the shrinkage of the optic tract ipsilateral to the lesion as an indirect measure of RTSD showed that patients with minimal optic tract lateralisation achieved greater visual field recovery than those with pronounced shrinkage [74]. Therefore, patients with relatively preserved cells in the affected hemiretina should be better candidates for intensive vision restoration training. In contrast, in cases of profound ganglion loss, compensatory strategies should be considered.

5 | Conclusion

The available evidence indicates that post-chiasmatic stroke induces retinal degeneration, affecting both peripapillary and macular layers. Even if some variability exists across studies, for example, in pRNFL findings or correlations with visual field defect, these differences may be due to methodological heterogeneity, sample characteristics, and the timing of OCT assessment. Macular indices, given the stronger topographic correspondence with the visual field defect and their lower susceptibility to confounding factors, represent the most consistent measure of RTSD and should therefore be preferred over the peripapillary measures. All together, the present findings support the use of OCT as a reliable structural biomarker of post-geniculate neuronal loss and as a potential predictor of visual function recovery. Multicentric, longitudinal studies employing standardized OCT protocols and integrated functional assessments are warranted to refine our understanding of RTSD dynamics, clarify its prognostic implications, and guide the development of targeted neuroprotective and rehabilitative interventions.

Author Contributions

F.C.: Conceptualization, methodology, investigation, data curation, visualization, writing – original draft. G.G.: Conceptualization, methodology, investigation, data curation, visualization, writing – original draft. L.M.: Writing – review and editing. S.B.M.: Supervision resources, writing – review and editing. N.B.: Supervision, conceptualization, resources, funding acquisition, writing – review and editing.

Acknowledgements

Open access publishing facilitated by Universita degli Studi di Milano-Bicocca, as part of the Wiley - CRUI-CARE agreement.

Funding

This work was supported by Italian Ministry of Health, Ricerca Corrente (to N.B.).

Conflicts of Interest

The authors declare no conflicts of interest.

Data Availability Statement

Data sharing not applicable to this article as no datasets were generated or analysed during the current study.

References

1. V. L. Feigin, B. A. Stark, C. O. Johnson, et al., "Global, Regional, and National Burden of Stroke and Its Risk Factors, 1990–2019: A Systematic Analysis for the Global Burden of Disease Study 2019," *Lancet Neurology* 20, no. 10 (2021): 795–820, https://doi.org/10.1016/S1474-4422(21)00252-0.

2. A. Pollock, C. Hazelton, J. F. Rowe, et al., "Interventions for Visual Field Defects in People With Stroke (Review) Interventions for Visual Field Defects in People With Stroke (Review)," *Cochrane Library Cochrane Database of Systematic Reviews* 5 (2019): CD008388, https://doi.org/10.1002/14651858.CD008388.pub3.

3. S. Tol, G. A. de Haan, E. M. J. L. Postuma, J. L. Jansen, and J. Heutink, "Reading Difficulties in Individuals With Homonymous Visual Field Defects: A Systematic Review of Reported Interventions," *Neuropsychology Review* 35, no. 2 (2025): 254–300, https://doi.org/10.1007/s11065-024-09636-4.

4. H. Bridge, P. Jindahra, J. Barbur, and G. T. Plant, "Imaging Reveals Optic Tract Degeneration in Hemianopia," *Investigative Ophthalmology & Visual Science* 52, no. 1 (2011): 382–388, https://doi.org/10.1167/iovs.10-5708.

5. R. M. Beatty, A. A. Sadun, L. Smith, J. P. Vonsattel, and E. P. Richardson, "Direct Demonstration of Transsynaptic Degeneration in the Human Visual System: A Comparison of Retrograde and Anterograde Changes," *Journal of Neurology, Neurosurgery & Psychiatry* vol. 45 (1982).

6. A. Cowey, I. Alexander, and P. Stoerig, "Transneuronal Retrograde Degeneration of Retinal Ganglion Cells and Optic Tract in Hemianopic Monkeys and Humans," *A Journal of Neurology* 134 (2011): 2149–2157, https://doi.org/10.1093/brain/awr125.

7. C. L. Schneider, E. K. Prentiss, A. Busza, et al., "Survival of Retinal Ganglion Cells After Damage to the Occipital Lobe in Humans Is Activity Dependent," *Proceedings of the Royal Society B: Biological Sciences* 286, no. 1897 (2019), https://doi.org/10.1098/rspb.2018.2733.

8. H. Johnson and A. Cowey, "Transneuronal Retrograde Degeneration of Retinal Ganglion Cells Following Restricted Lesions of Striate Cortex in the Monkey," *Experimental Brain Research* 132, no. 2 (2000): 269–275, https://doi.org/10.1007/S002210000384/METRICS.

9. J. M. Van Buren, "Trans-Synaptic Retrograde Degeneration in the Visual System of Primates," *Journal of Neurology, Neurosurgery, and Psychiatry* 26 (1963): 402–409.

10. N. R. Miller and S. A. Newman, "Transsynaptic Degeneration," *Archives of Ophthalmology* 99, no. 9 (1981): 1654, https://doi.org/10.1001/archopht.1981.03930020528032.

11. D. Huang, E. A. Swanson, C. P. Lin, et al., "Optical Coherence Tomography," *Science* 254, no. 5035 (1991): 1178–1181, https://doi.org/10.1126/SCIENCE.1957169.

12. P. Jindahra, A. Petrie, and G. T. Plant, "Retrograde Trans-Synaptic Retinal Ganglion Cell Loss Identified by Optical Coherence Tomography," *Brain* 132, no. 3 (2009): 628–634, https://doi.org/10.1093/brain/awp001.

13. J. I. Lee, L. Boerker, L. Gemerzki, et al., "Retinal Changes After Posterior Cerebral Artery Infarctions Display Different Patterns of the Nasal Und Temporal Sector in a Case Series," *Frontiers in Neurology* 11 (2020): 11, https://doi.org/10.3389/fneur.2020.00508.

14. J. S. Xie, L. Donaldson, and E. Margolin, "The Use of Optical Coherence Tomography in Neurology: A Review," *Brain. Oxford University Press* 145, no. 12 (2022): 4160–4177, https://doi.org/10.1093/brain/awac317.

15. W. Drexler and J. Fujimoto, "State-Of-The-Art Retinal Optical Coherence Tomography," *Progress in Retinal and Eye Research* 27, no. 1 (2008): 45–88, https://doi.org/10.1016/j.preteyeres.2007.07.005.

16. N. Minakaran, E. R. de Carvalho, A. Petzold, and S. H. Wong, "Optical Coherence Tomography (OCT) in Neuro-Ophthalmology," *Eye (Basingstoke). Springer Nature* 35, no. 1 (2021): 17–32, https://doi.org/10.1038/s41433-020-01288-x.

17. O. Mirmosayyeb, R. Zivadinov, B. Weinstock-Guttman, R. H. B. Benedict, and D. Jakimovski, "Optical Coherence Tomography (OCT) Measurements and Cognitive Performance in Multiple Sclerosis: A Systematic Review and Meta-Analysis," *Journal of Neurology. Springer Science and Business Media Deutschland GmbH* 270, no. 3 (2023): 1266–1285, https://doi.org/10.1007/s00415-022-11449-5.

18. V. T. T. Chan, Z. Sun, S. Tang, et al., "Spectral-Domain OCT Measurements in Alzheimer's Disease," *Ophthalmology* 126, no. 4 (2019): 497–510, https://doi.org/10.1016/j.ophtha.2018.08.009.

19. C. Y. l. Cheung, M. K. Ikram, C. Chen, and T. Y. Wong, "Imaging Retina to Study Dementia and Stroke," *Progress in Retinal and Eye Research* 57 (2017): 89–107, https://doi.org/10.1016/j.preteyeres.2017.01.001.

20. M. Ouzzani, H. Hammady, Z. Fedorowicz, and A. Elmagarmid, "Rayyan—A Web and Mobile App for Systematic Reviews," *Systematic Reviews* 5, no. 1 (2016): 210, https://doi.org/10.1186/s13643-016-0384-4.

21. M. J. Page, J. E. McKenzie, P. M. Bossuyt, et al., "The PRISMA 2020 Statement: An Updated Guideline for Reporting Systematic Reviews," *PLoS Medicine* 18, no. 3 (2021): e1003583, https://doi.org/10.1371/journal.pmed.1003583.

22. R. Anjos, L. Vieira, L. Costa, et al., "Macular Ganglion Cell Layer and Peripapillary Retinal Nerve Fibre Layer Thickness in Patients With Unilateral Posterior Cerebral Artery Ischaemic Lesion: An Optical Coherence Tomography Study," *Neuro-Ophthalmology* 40, no. 1 (2016): 8–15, https://doi.org/10.3109/01658107.2015.1122814.

23. K. Goto, A. Miki, T. Yamashita, et al., "Sectoral Analysis of the Retinal Nerve Fiber Layer Thinning and Its Association With Visual Field Loss in Homonymous Hemianopia Caused by Post-Geniculate Lesions Using Spectral-Domain Optical Coherence Tomography," *Graefe's Archive for Clinical and Experimental Ophthalmology* 254, no. 4 (2016): 745–756, https://doi.org/10.1007/s00417-015-3181-1.

24. A. Gunes, E. E. Inal, S. Demirci, L. Tok, O. Tok, and S. Demirci, "Changes in Retinal Nerve Fiber Layer Thickness in Patients With Cerebral Infarction: Evidence of Transneuronal Retrograde Degeneration," *Acta Neurologica Belgica* 116, no. 4 (2016): 461–466, https://doi.org/10.1007/s13760-015-0592-z.

25. H. Y. L. Park, Y. G. Park, A. H. Cho, and C. K. Park, "Transneuronal Retrograde Degeneration of the Retinal Ganglion Cells in Patients With Cerebral Infarction," *Ophthalmology* 120, no. 6 (2013): 1292–1299, https://doi.org/10.1016/j.ophtha.2012.11.021.

26. R. Pan, C. Ye, Z. Zhang, et al., "Distinct Alterations of Retinal Structure Between Thalamic and Extra-Thalamic Subcortical Infarction Patients: A Cross-Sectional and Longitudinal Study," *CNS Neuroscience & Therapeutics* 30, no. 4 (2024): e14543, https://doi.org/10.1111/cns.14543.

27. A. S. Rashid, D. Rashid, G. Yang, H. Link, H. Gauffin, and Y. Huang-Link, "Homonymous Visual Field Defect and Retinal Thinning After Occipital Stroke," *Brain and Behavior: A Cognitive Neuroscience Perspective* 11, no. 10 (2021): e2345, https://doi.org/10.1002/brb3.2345.

28. T. Yamashita, A. Miki, Y. Iguchi, K. Kimura, F. Maeda, and J. Kiryu, "Reduced Retinal Ganglion Cell Complex Thickness in Patients With Posterior Cerebral Artery Infarction Detected Using Spectral-Domain Optical Coherence Tomography," *Japanese Journal of Ophthalmology* 56, no. 5 (2012): 502–510, https://doi.org/10.1007/s10384-012-0146-3.

29. T. Yamashita, A. Miki, K. Goto, et al., "Retinal Ganglion Cell Atrophy in Homonymous Hemianopia due to Acquired Occipital Lesions Observed Using Cirrus High-Definition-OCT," *Journal of Ophthalmology* 2016 (2016): 1–9, https://doi.org/10.1155/2016/2394957.

30. C. Ye, W. R. Kwapong, W. Tao, et al., "Alterations of Optic Tract and Retinal Structure in Patients After Thalamic Stroke," *Frontiers in Aging Neuroscience* 14 (2022): 14, https://doi.org/10.3389/fnagi.2022.942438.

31. A. Eshtiaghi and J. A. Micieli, "Rapid Homonymous Hemi-Macular Atrophy of the Optical Coherence Tomography Ganglion Cell Complex After Stroke," *BMJ Case Reports* 14, no. 4 (2021): e241967, https://doi.org/10.1136/bcr-2021-241967.

32. S. Bianchi Marzoli, L. Melzi, P. Ciasca, et al., "Quantification of Retinal Ganglion Cell Loss in Patients With Homonymous Visual Field Defect due to Stroke," *Neurological Sciences* 44, no. 8 (2023): 2811–2819, https://doi.org/10.1007/s10072-023-06675-2.

33. A. Herro and B. Lam, "Retrograde Degeneration of Retinal Ganglion Cells in Homonymous Hemianopsia," *Clinical Ophthalmology* 9 (2015): 1057–1064, https://doi.org/10.2147/OPTH.S81749.

34. M. R. Cavanaugh, L. M. Blanchard, M. McDermott, B. L. Lam, M. Tamhankar, and S. E. Feldon, "Efficacy of Visual Retraining in the Hemianopic Field After Stroke: Results of a Randomized Clinical Trial," *Ophthalmology* 128, no. 7 (2021): 1091–1101, https://doi.org/10.1016/j.ophtha.2020.11.020.

35. X. Bai, L. Cao, H. Wang, et al., "Retinal Thickness Is Indicative of Visual Loss in Patients With Occipital Lobe Infarction," *Frontiers in Neurology* 16 (2025): 1546439, https://doi.org/10.3389/fneur.2025.1546439.

36. Y. Liang, B. Liu, Y. Xiao, et al., "Retinal Neurovascular Changes in Patients With Ischemic Stroke Investigated by Optical Coherence Tomography Angiography," *Frontiers in Aging Neuroscience* 14 (2022): 14, https://doi.org/10.3389/fnagi.2022.834560.

37. S. G. Schwartz, A. Monroig, and H. W. Flynn, "Progression of Transsynaptic Retinal Degeneration With Spectral-Domain Optical Coherence Tomography," *American Journal of Ophthalmology Case Reports* 5 (2017): 67–72, https://doi.org/10.1016/J.AJOC.2016.12.010.

38. J. A. Micieli, R. J. Blanch, and K. Narayana, "Teaching NeuroImages: Evolving Trans-Synaptic Degeneration of Retinal Ganglion Cells After Occipital Lobe Stroke," *Neurology* 90, no. 24 (2018): e2174–e2178, https://doi.org/10.1212/WNL.0000000000005686.

39. L. Donaldson, M. Chen, and E. Margolin, "Transsynaptic Ganglion Cell Degeneration in Adult Patients After Occipital Lobe Stroke," *Journal of Neuro-Ophthalmology* 43, no. 2 (2023): 243–247, https://doi.org/10.1097/WNO.0000000000001657.

40. P. Jindahra, A. Petrie, and G. T. Plant, "The Time Course of Retrograde Trans-Synaptic Degeneration Following Occipital Lobe Damage in Humans," *Brain* 135, no. 2 (2012): 534–541, https://doi.org/10.1093/brain/awr324.

41. T. Yamashita, A. Miki, K. Goto, et al., "Evaluation of Significance Maps and the Analysis of the Longitudinal Time Course of the Macular Ganglion Cell Complex Thicknesses in Acquired Occipital Homonymous Hemianopia Using Spectral-Domain Optical Coherence Tomography," *Neuro-Ophthalmology* 44, no. 4 (2020): 236–245, https://doi.org/10.1080/01658107.2019.1686764.

42. B. K. Fahrenthold, M. R. Cavanaugh, M. Tamhankar, et al., "Training in Cortically Blinded Fields Appears to Confer Patient-Specific Benefit Against Retinal Thinning," *Investigative Ophthalmology & Visual Science* 65, no. 4 (2024): 29, https://doi.org/10.1167/iovs.65.4.29.

43. H. Wässle, "Parallel Processing in the Mammalian Retina," *Nature Reviews Neuroscience* 5, no. 10 (2004): 747–757, https://doi.org/10.1038/NRN1497.

44. Y. J. Kim, M. H. Kang, H. Y. Cho, H. W. Lim, and M. Seong, "Comparative Study of Macular Ganglion Cell Complex Thickness Measured by Spectral-Domain Optical Coherence Tomography in Healthy Eyes, Eyes With Preperimetric Glaucoma, and Eyes With Early Glaucoma," *Japanese Journal of Ophthalmology* 58, no. 3 (2014): 244–251, https://doi.org/10.1007/S10384-014-0315-7.

45. F. Mühlemann, H. Grabe, A. Fok, et al., "Homonymous Hemiatrophy of Ganglion Cell Layer From Retrochiasmal Lesions in the Visual Pathway," *Neurology* 94, no. 3 (2020): E323–E329, https://doi.org/10.1212/WNL.0000000000008738.

46. P. H. Schiller and J. G. Malpeli, "Functional Specificity of Lateral Geniculate Nucleus Laminae of the Rhesus Monkey," *Journal of Neurophysiology* 41, no. 3 (1978): 788–797, https://doi.org/10.1152/jn.1978.41.3.788.

47. V. H. Perry, R. Oehler, and A. Cowey, "Retinal Ganglion Cells That Project to the Dorsal Lateral Geniculate Nucleus in the Macaque Monkey," *Neuroscience* 12, no. 4 (1984): 1101–1123, https://doi.org/10.1016/0306-4522(84)90006-X.

48. A. Prasannakumar, V. Kumar, P. Mailankody, et al., "A Systematic Review and Meta-Analysis of Optical Coherence Tomography Studies in Schizophrenia, Bipolar Disorder and Major Depressive Disorder," *World Journal of Biological Psychiatry* 24, no. 8 (2023): 707–720, https://doi.org/10.1080/15622975.2023.2203231.

49. R. E. Weller and J. H. Kaas, "Parameters Affecting the Loss of Ganglion Cells of the Retina Following Ablations of Striate Cortex in Primates," *Visual Neuroscience* 3, no. 4 (1989): 327–349, https://doi.org/10.1017/S0952523800005514.

50. A. Cowey, P. Stoerig, and V. H. Perry, "Transneuronal Retrograde Degeneration of Retinal Ganglion Cells After Damage to Striate Cortex in Macaque Monkeys: Selective Loss of Pβ Cells," *Neuroscience* 29, no. 1 (1989): 65–80, https://doi.org/10.1016/0306-4522(89)90333-3.

51. E. L. Saionz, M. R. Cavanaugh, B. A. Johnson, D. Harrington, G. K. Aguirre, and K. R. Huxlin, "Evolution of Visual Field Defects After Occipital Stroke: A Quantitative Analysis," *Translational Vision Science & Technology* 14, no. 6 (2025): 14, https://doi.org/10.1167/tvst.14.6.14.

52. X. Zhang, S. Kedar, M. J. Lynn, N. J. Newman, and V. Biousse, "Homonymous Hemianopias," *Neurology* 66, no. 6 (2006): 906–910, https://doi.org/10.1212/01.wnl.0000203913.12088.93.

53. M. Dinkin, "Trans-Synaptic Retrograde Degeneration in the Human Visual System: Slow, Silent, and Real," *Current Neurology and Neuroscience Reports* 17, no. 2 (2017): 16, https://doi.org/10.1007/s11910-017-0725-2.

54. J. Shen, Y. Wang, and K. Yao, "Protection of Retinal Ganglion Cells in Glaucoma: Current Status and Future," *Experimental Eye Research* 205 (2021): 108506, https://doi.org/10.1016/j.exer.2021.108506.

55. S. Trauzettel-Klosinski, "Current Methods of Visual Rehabilitation," *Deutsches Ärzteblatt International* 108, no. 29–30 (2011): 519–525, https://doi.org/10.3238/arztebl.2011.0871.

56. T. M. Schofield and A. P. Leff, "Rehabilitation of Hemianopia," *Current Opinion in Neurology* 22, no. 1 (2009): 36–40, https://doi.org/10.1097/WCO.0b013e32831f1b2c.

57. E. Kasten, S. Wüst, W. Behrens-Baumann, and B. A. Sabel, "Computer-Based Training for the Treatment of Partial Blindness," *Nature Medicine* 4, no. 9 (1998): 1083–1087, https://doi.org/10.1038/2079.

58. B. A. Sabel, P. Henrich-Noack, A. Fedorov, and C. Gall, "Vision Restoration After Brain and Retina Damage: The "Residual Vision Activation Theory."," in *Progress in Brain Research*, vol. 192 (Elsevier B.V., 2011), 199–262, https://doi.org/10.1016/B978-0-444-53355-5.00013-0.

59. B. A. Sabel, S. Kenkel, and E. Kasten, "Vision Restoration Therapy (VRT) Efficacy as Assessed by Comparative Perimetric Analysis and Subjective Questionnaires," *Restorative Neurology and Neuroscience* 22, no. 6 (2004): 399–420.

60. G. Kerkhoff, U. Münßinger, E. Haaf, G. Eberle-Strauss, and E. Stögerer, "Rehabilitation of Homonymous Scotomata in Patients With Postgeniculate Damage of the Visual System: Saccadic Compensation Training," *Restorative Neurology and Neuroscience* 4, no. 4 (1992): 245–254, https://doi.org/10.3233/RNN-1992-4402.

61. J. Zihl, "Visual Scanning Behavior in Patients With Homonymous Hemianopia," *Neuropsychologia* 33, no. 3 (1995): 287–303, https://doi.org/10.1016/0028-3932(94)00119-A.

62. A. L. M. Pambakian, "Saccadic Visual Search Training: A Treatment for Patients With Homonymous Hemianopia," *Journal of Neurology, Neurosurgery & Psychiatry* 75, no. 10 (2004): 1443–1448, https://doi.org/10.1136/jnnp.2003.025957.

63. N. Bolognini, F. Frassinetti, A. Serino, and E. Làdavas, ""Acoustical Vision" of Below Threshold Stimuli: Interaction Among Spatially Converging Audiovisual Inputs," *Experimental Brain Research* 160, no. 3 (2005): 273–282, https://doi.org/10.1007/s00221-004-2005-z.

64. N. Bolognini, L. Diana, A. Rossetti, et al., "Telerehabilitation for Visual Field Defects With a Multisensory Training: A Feasibility Study," *Journal of Neuroengineering and Rehabilitation* 22, no. 1 (2025): 34, https://doi.org/10.1186/s12984-025-01573-4.

65. C. Perin, B. Vigano, D. Piscitelli, B. M. Matteo, R. Meroni, and C. G. Cerri, "Non-Invasive Current Stimulation in Vision Recovery: A Review of the Literature," *Restorative Neurology and Neuroscience* 38, no. 3 (2020): 239–250, https://doi.org/10.3233/RNN-190948.

66. L. Diana, C. Casati, L. Melzi, S. B. Marzoli, and N. Bolognini, "Enhancing Multisensory Rehabilitation of Visual Field Defects With Transcranial Direct Current Stimulation: A Randomized Clinical Trial," *European Journal of Neurology* 32, no. 1 (2024): e16559, https://doi.org/10.1111/ene.16559.

67. E. Raffin, M. Bevilacqua, F. Windel, et al., "Boosting Hemianopia Recovery: The Power of Interareal Cross-Frequency Brain Stimulation," *Brain* 148, no. 12 (2025): 4548–4561, https://doi.org/10.1093/brain/awaf252.

68. F. Herpich, M. D. Melnick, S. Agosta, K. R. Huxlin, D. Tadin, and L. Battelli, "Behavioral/Cognitive Boosting Learning Efficacy with Noninvasive Brain Stimulation in Intact and Brain-Damaged Humans," 39, no. 28 (2019), 5551–5561, https://doi.org/10.1523/JNEUROSCI.3248-18.2019.

69. M. Bevilacqua, F. Windel, E. Beanato, et al., "Pathway-Dependent Brain Stimulation Responses Indicate Motion Processing Integrity After Stroke," *Brain* 148, no. 7 (2025): 2361–2372, https://doi.org/10.1093/brain/awaf043.

70. M. M. Carlà, M. Ripa, E. Crincoli, F. Catania, and S. Rizzo, "The Spectrum of Microcystic Macular Edema: Pathogenetic Insights, Clinical Entities, and Functional Prognosis," *Survey of Ophthalmology* 70, no. 5 (2025): 982–994, https://doi.org/10.1016/j.survophthal.2025.03.010.

71. H. Y. Shin, H. Y. L. Park, J. A. Choi, and C. K. Park, "Macular Ganglion Cell–Inner Plexiform Layer Thinning in Patients With Visual Field Defect That Respects the Vertical Meridian," *Graefe's Archive for Clinical and Experimental Ophthalmology* 252, no. 9 (2014): 1501–1507, https://doi.org/10.1007/s00417-014-2706-3.

72. J. Keller, B. F. Sánchez-Dalmau, and P. Villoslada, "Lesions in the Posterior Visual Pathway Promote Trans-Synaptic Degeneration of Retinal Ganglion Cells," *PLoS One* 9, no. 5 (2014): e97444, https://doi.org/10.1371/journal.pone.0097444.

73. S. Zehnder, H. Wildberger, J. V. M. Hanson, et al., "Retinal Ganglion Cell Topography in Patients With Visual Pathway Pathology," *Journal of*

Neuro-Ophthalmology 38, no. 2 (2018): 172–178, https://doi.org/10.1097/WNO.0000000000000589.

74. B. K. Fahrenthold, M. R. Cavanaugh, S. Jang, et al., "Optic Tract Shrinkage Limits Visual Restoration After Occipital Stroke," *Stroke* 52, no. 11 (2021): 3642–3650, https://doi.org/10.1161/STROKEAHA.121.034738.

Supporting Information

Additional supporting information can be found online in the Supporting Information section. **Data S1:** ene70566-sup-0001-Supinfo01.docx. **Table S1:** Overview of studies and the retinal layer variables they measured. "+" indicates that the study extracted the variable "–" indicates it was not considered and "N/A" indicates data not available. Variables include: peripapillary retinal nerve fiber layer (pRNFL), macular retinal nerve fiber layer (mRNFL), ganglion cell layer (GCL), ganglion cell–inner plexiform layer (GC-IPL), ganglion cell complex (GCC), inner retinal layers (IRL), and global and local volumetric measures (GLV/FLV). **Table S2:** Sectoral analysis of OCT parameters. Sectoral measurements of retinal layer thickness in control and stroke patients across studies. When available, values are reported as mean ± SD. Data are divided by quadrants or sectors according to each study's segmentation. Columns indicate the right/left eye, ipsilateral/contralateral eye, symptomatic/asymptomatic visual field, anterior/posterior lesions, and time point evaluations when available. pRNFL, peripapillary Retinal Nerve Fiber Layer; mRNFL, macular Retinal Nerve Fiber Layer; GC-IPL, Ganglion Cell–Inner Plexiform Layer; GCC, Ganglion Cell Complex; IRL, Inner Retinal Layers; FLV, Focal Loss Volume; GLV, Global Loss Volume; S, superior; ST, superior temporal; TS, temporal superior; T, temporal; TU, temporal upper; TL, temporal lower; IT, inferior temporal; I, inferior; IN, inferior nasal; NI, nasal inferior; N, nasal; NL, nasal lower; NU, nasal upper; SN, superior nasal; VFD, visual field defect; NVFD, non-visual field defect; T0/T1/T2, time-points assessment.